

Effect of pine bark biochar on the vertical morphological transformation of soil heavy metals

Zhu Xinyu¹, Yao Wen¹, Ji Zhenxiang¹, Hou Yumei¹

¹Faculty of Environment and Architecture, University of Shanghai for Science and Technology, Shanghai 200093, China

Abstract

Pine bark biochar was selected from two different preparation temperatures (300 °C and 600 °C) and characterized by X-ray diffraction (XRD) and Fourier transform infrared spectroscopy (FTIR). The morphological distribution and vertical transport characteristics of heavy metals Cr and Cd were investigated under simulated acid rain leaching conditions for the remediation of soil.

The experimental results showed that biochar treatment of soil can effectively reduce the content of exchangeable state and carbonate state of heavy metals Cr and Cd, which is conducive to the conversion to more stable metal forms and reduce the migration activity in the soil. The characterization results showed that the high-temperature biochar contains more ash and specific surface area, while the low-temperature biochar contains more functional groups, which are more favorable for complexation and adsorption with heavy metals. Combined with the drenching experiments and related literature, it was found that although acid rain could enhance the mobility of soil heavy metals, the addition of biochar reduced this mobility to a greater extent, especially the low-temperature biochar PB300, which contributed significantly to the morphological conversion of heavy metals as well as the reduction of longitudinal migration of heavy metals, and could better reduce the effects caused by acid rain.

Keywords: Heavy Metals, Pine Bark Biochar, Stabilization, Metal form distribution

Date of Submission: 11-02-2023

Date of acceptance: 24-02-2023

I. INTRODUCTION

Soil plays a crucial role in the security and stability of society and is a very major reservoir of nutrients and contaminants. Nevertheless, with the economic and social progress, factors such as rock weathering, ore refining, fertilizers and pesticides use, electroplating application and other natural or artificial factors will lead to the entrance of various heavy metals, increasing the concentration of heavy metals in the soil and leading to soil pollution [1]. Heavy metals (HMs) seriously affect environmental quality, food safety and human healthy due to its persistent, mobile, phytotoxic, bioaccumulative and non-degradable nature [2]. Especially, geological and anthropogenic activities caused excessive release of Cr, Cd and other heavy metals into the soil, which increases the risk to human health through accumulation in the food chain. Especially in acid rain areas [3]. When acid rain falls into the soil, the soil's properties change, which leads to nutrient leaching out of the soil. As the flux of SO₄²⁻ in acid rain increases, it leads to the equipotential leaching of hydrogen ions and other cations, where heavy metals are more likely to be activated and released into the soil, leading to a further environmental risk. In general, acid rain can alter soil properties, reduce soil fertility, and increase the toxicity of heavy metals present in the system, making soil heavy metal pollution in the Yangtze River Delta even more severe[4]. Therefore, in order to achieve the target of sustainable property development, investigating efficient and safe soil improvement methods to the immobilization of heavy metals in soil under long-term acid rain threat is becoming the preferred in situ remediation technology.

Various methods are available for remediation of heavy metal contaminated soils. The remediation of contaminated sites by physico-chemical methods, micromediation and phytoremediation has been widely studied and discussed. Including soil modification method, electrode method and microbial activity method, etc. [5]. Yet these methods usually have the disadvantages of being costly and unwieldy. Thus, finding a simple, convenient and efficient remediation method becomes imperative.

In-situ passivation method has the advantage of effective remediation, short-term remediation period, low-cost and simply operation, which has a high potential research value in the remediation of heavy metal contaminated soil [6]. Of which, biochar was regarded as an economic and eco-friendly remediation strategy for heavy metal contamination [7]. Biochar is a carbon-rich material obtained from the combustion of organic raw materials under an oxygen limited condition with a certain temperature[8]. With the advantages of enriched carbon content, large specific surface area and high cation exchange capacity, biochar is commonly used in

remediation research of heavy metal contaminated soil [9]. The chemical and physical properties of biochar vary dramatically depending on the raw material and production conditions [10]. Plenty of studies have proved that the application of biochar in heavy metal contaminated soil shows favorable effects on the stabilization of metals. Li et al.[11] prepared a novel composite rice-hull biochar material for the passivation remediation of Cd-contaminated soil, which significantly enhanced the chemical stability of Cd in the soil. Liao et al.[12] formulated biochar & zeolite amendments for the immobilization of heavy metals such as Pb and Cd in soil to effectively prevent the leakage of heavy metals from contaminated soil. Tao et al.[13] used modified zeolite to improve the leaching effect of soil Pb and Zn, showing that adding zeolite can effectively prevent the leakage of heavy metals from soil under acid rain conditions. Hu et al.[14] showed that in agricultural areas contaminated with heavy metal Pb, where there are also perennial heavy rainfall or moderate or above acid rain, the amount of Pb leaching from the soil with rainwater will also be increased. However, few studies on the long-term stability evaluation of biochar in in-situ remediation technology, as well as the morphological distribution or vertical transport of heavy metals in soil have been conducted.

Accordingly, this paper uses pine bark as the raw material with two different preparation temperatures (300°C and 600°C) for remediation of heavy metals Cr and Cd in soil under simulated acid rain leaching, so as to explore the patterns of morphological transformation and vertical migration of Cr and Cd in soil by using biochar. Combined with leaching experiments to analyze the passivation effect, the results were equally relevant for the biochar preparation and groundwater impermeation.

II. MATERIALS AND METHODS

2.1 Soil collection and incubation experiments

Soil samples were collected from an open vegetable field at a facility in Xixin Town, Chongming District, Shanghai, and the contents of heavy metals are shown in Table 1. It can be found from the table shows that the pollution level of heavy metal contaminated soil is 3.64 times and 105.58 times of the standard value, respectively, with reference to the Environmental quality standard for soils. Firstly, 1 kg of soil samples weighed, weeded out plant roots, stones and other debris, and placed in the incubator; then, aqueous liquids containing 2828.65 mg K₂Cr₂O₄ and 658.51 mg Cd(NO₃)₂·4H₂O were respectively added to the soil and incubated for 60 days at constant temperature avoiding light; finally, the aged soil samples were naturally air-dried and passed through 10 mesh quasi-nylon sieve to obtain the Cr and Cd contaminated soil samples, respectively. The constant temperature (25°C) and water content (70% of maximum water holding capacity) were maintained throughout the experiment.

Table 1:Cr and Cd in Shanghai topsoil

Elements (mg/kg)	Min.	Med.	Max.	Arithmetic mean±sd	Geometric mean ± sd
Cr	37.30	73.80	87.90	70.20±14.49	68.50±1.28
Cd	±0.05	0.13	0.33	0.14±0.07	0.12±1.60

2.2 Biochar preparation and characterization

Biochar is prepared from pine bark. Pine bark was firstly washed with deionized water, dried and crushed, then loaded into a ceramic crucible and wrapped with aluminum foil, final heated in a muffle furnace. Choose two lysis temperatures, 300 and 600 °C, for 5h. Cooled to room temperature, removed, crushed, passed through a 20 mesh standard nylon sieve, and stored in a self-sealing bag for backup, marked as PB300 and PB600.

Biochar physicochemical properties, including pH, particle size, ash, C H N O content, sample structural composition, and surface functional groups, were analyzed by potentiometry, laser particle size distribution (Bettersize 2000E, Baxter Instruments, Dandong), muffle heating, elemental analyzer (vario MACRO cube, Elementar, Germany), X-ray Diffractometer (FTIR), and Fourier Transform Infrared Spectrometer (FTIR). Diffractometer and Fourier Transform Infrared Spectrometer (FTIR). In addition, particle size, morphology, mineralogy, and surface area were analyzed by sieve analysis, scanning electron microscopy (SEM) equipped with energy dispersive X-ray spectroscopy (Philips Leo 1455 V P), X-ray diffraction (XRD; PW 3040 V60, X'Pert Pro MPD), and Brunauer -Emmett-Teller surface area analyzer (Micromeritics TriStar II) were used for the determination.

2.3 Leaching device design and operation

The leach test was performed using the simulated soil column method, and the leach test device (Plexiglas tube: 50 cm high, 2.9 cm diameter) is shown in Figure 1. The prepared PB300 and PB600 biochar were uniformly added into the soil samples contaminated with heavy metals Cr and Cd at 5% mixing ratio, and the soil samples without biochar added were set as blank control group, and each treatment was repeated three

times. Before adding the soil, the bottom of the column is sealed with a No. 6 rubber plug and a 1 cm thick layer of coarse quartz sand is spread to prevent soil loss and outlet blockage. Applying a layer of petroleum jelly to the inner surface of the column to avoid water running down the column walls. The lower 20 cm of the column is laid with original clean soil and the upper 20 cm with contaminated soil. For each 2 cm of soil added to the column, compact the soil with a grinding rod after each addition to ensure that the soil capacity in its natural condition is reached. A 2mm latex tube is perforated with a rubber plug at the lower end of the soil column to collect the filtrate. Fill the soil column with soil sample and set it with iron frame table.

According to the average pH of acid rain in Shanghai with ionic composition, in this experiment, the pH of acid rain drench solution was 5.12, which was configured by deionized water containing H₂SO₄ and 1×10⁻⁴ molL⁻¹ of HNO₃ at a concentration of 4×10⁻⁴ molL⁻¹. The leachate was added every 3 days for 60 days, and a total of 1 L of leachate was consumed. The column was wetted with 300 mL of deionized water before leaching and left to incubate for 3 to 5 days. Leachate for analysis was collected at regular intervals from the lower part of the soil column in thin-mouthed bottles. The experiments were conducted at ambient temperature and under laboratory conditions, In order to reduce the error, two parallel samples were used for each. The results were averaged.

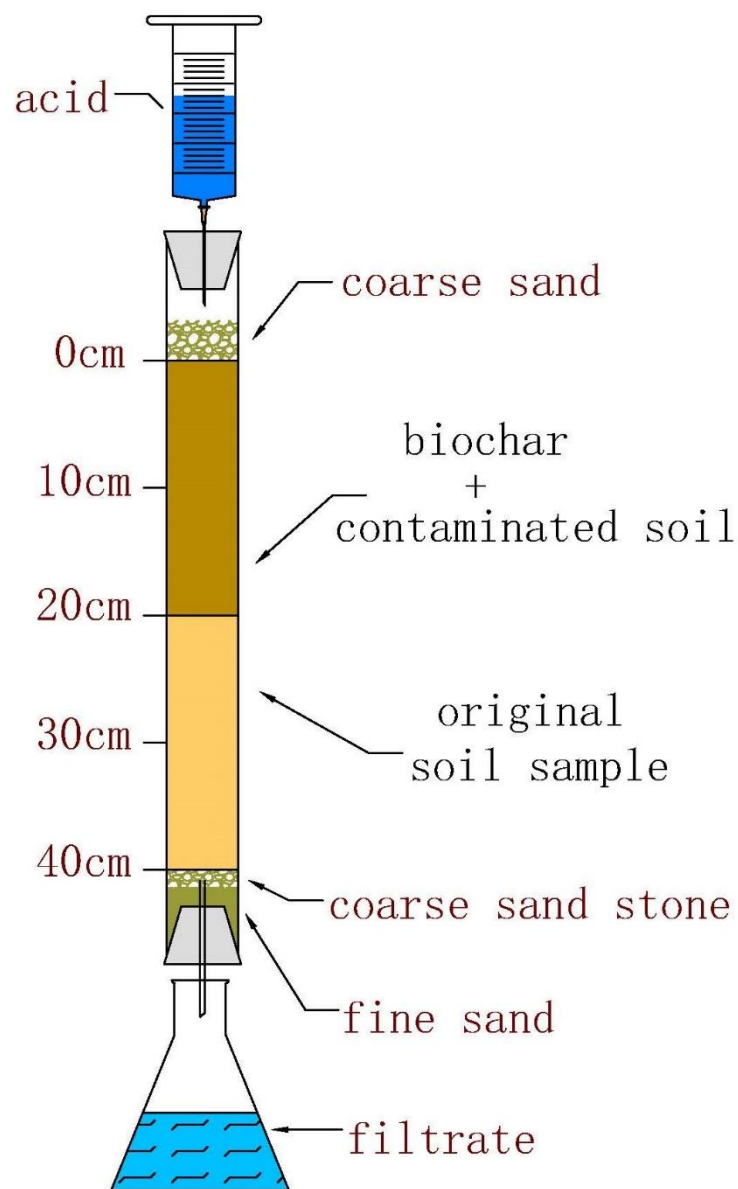


Figure1: Leaching experimental device

2.4 Sequential chemical extraction

Tessier et al. [15] proposed a continuous extraction scheme that can be used to assess the distribution of PTEs in soils. After drying and passing the soil sample through 10 mesh sieve, 2.5g of soil sample was weighed for three extractions. Afterward the following operationally definable hierarchy of PTEs was obtained. **Exchangeable (EXC)**: Soluble in 1 M MgCl₂, pH 7.0. **Bound to carbonates (Carb)**: dissolved in 1 M NaOAc, pH 5.0. **Bound to Fe-oxides (FeMnOx)**: 0.04 M NH₂OH/HCl dissolved in 25% acetic acid (v/v), pH 3.0. **Bound to Organic matter (OM)**: dissolved in 0.02 M HNO₃ + 30% H₂O₂, pH 2.0. soluble metal subsequently treated with 3.2 M NH₄OAC (v/v) in 20% HNO₃. **Residual (RES)**: The residue was dried, ground, and treated with acid for abatement. The samples of each component were sparged onto a 100 ml volumetric flask and analyzed by ICP-OES.

2.5 Determination of total heavy metals

The total amount of heavy metals Cr and Cd in soil samples were determined by the common four-acid digestion method (HCl-HNO₃-HF-HClO₄). Measure 0.3g of the sample in the digestion tank, wet it with a small amount of deionized water, add 15mL of concentrated hydrochloric acid, then put it into the graphite digestion apparatus, temperature control at about 100°C, and digest it in the ventilator. When the liquid in the digestion tank evaporates to about 2mL, remove from the digestion furnace and cool to ambient temperature. After that, 10mL of nitric acid, 10mL of hydrofluoric acid and 3mL of perchloric acid were added, with the temperature controlled at about 210°C, covered and disintegrated. At intervals, open the lid and shake the digestion tank to remove the resulting flying silica. When the white smoke of perchloric acid comes out from the digestion tank after a period of digestion, and when the black organic matter in the digestion tank disappears, opening the lid and driving away the white smoke. Until the bottom of the digestion tank is only a paste, remove the digestion tank and cool to ambient temperature. Flush the lid and interior of the digestion tank with 10% nitric acid to dissolve and digest the residue. Finally, cool and fix the contents in a 50mL volumetric flask. [16] The concentrations of heavy metals were determined with an Optima 8000 plasma inductively coupled emission spectrometer (ICP-OES) from PerkinElmer, USA, and the aqueous sediment standard (GSD-9) was selected as the sample quality control to calculate the content of heavy metals in soil.

III. RESULT AND DISCUSSION

3.1 Soil physicochemical properties

Soil pH measured by PHS-3C acidity meter was 7.79. The particle size distribution of the soil measured by the laser particle size distribution meter was 15.20% for sand, 79.41% for powder and 5.39% for clay, and the soil could be judged as loamy. Usually these soils are widely distributed in the middle and lower reaches of the Yangtze River, the river network plains of the Pearl River Delta and the alluvial plains on both sides of the river. The soil elemental analysis showed that the soil contains 1.71% carbon, 0.18% hydrogen and 0.58% nitrogen, which shows that the soil has a high organic matter content. The field water holding capacity of the soil was determined by the ring knife method [17] to be 30.6%, which shows that these soils are moderately sandy and sticky, with a proper ratio of large and small voids, good permeability, and high water and fertilizer retention capacity, making them a more desirable soil texture for agriculture.

The X-ray diffraction patterns of the original soil and the soil contaminated with heavy metals Cr and Cd measured by X-ray diffraction spectrometer are shown in Figure 2. The X-ray diffraction patterns of the original soil and the contaminated soil with heavy metals Cr and Cd measured by X-ray diffraction spectrometer are shown in Fig. 2. From the figure, it can be seen that there was no very obvious difference in the soil mineral structure between the Cr and Cd contaminated soils and the original soils, and the composition of these four types of soils is still dominated by SiO₂. But through the physical phase analysis, for the diffraction pattern of Cd-contaminated soil, weak additional peaks appear at 2 θ =5.7 and 26.3, which may have the generation of insoluble heavy metal minerals.

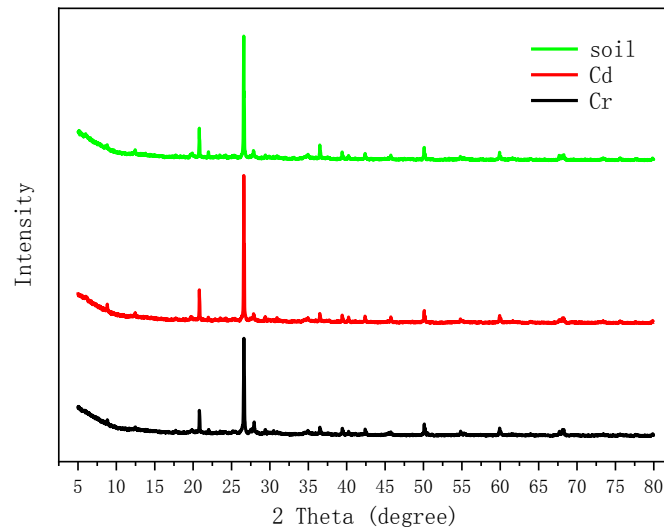


Figure 2: X-ray diffraction patterns of virgin soil and soil contaminated with heavy metals Cr and Cd

After the original soil was aged by Cr, Cd, the morphology of heavy metals was determined by the Tessier five-step extraction method, and the morphological distribution of heavy metals is shown in Figure 3. In the Cr-contaminated soil, the Cr content of each form is ranked as follows: EXC > Carb > FeMnOx > OM > RES, and the exchangeable state is the main form present in the soil, with a proportion of 36.6%. In Cd-contaminated soil, the order of distribution of each form was: EXC > FeMnOx > Carb > OM > Res, similar to the distribution in Cr-contaminated soil, but the content of FeMnOx was slightly higher than that of Carb. The proportion of Cd EXC distribution was 42%, which was slightly higher than that of Cr.

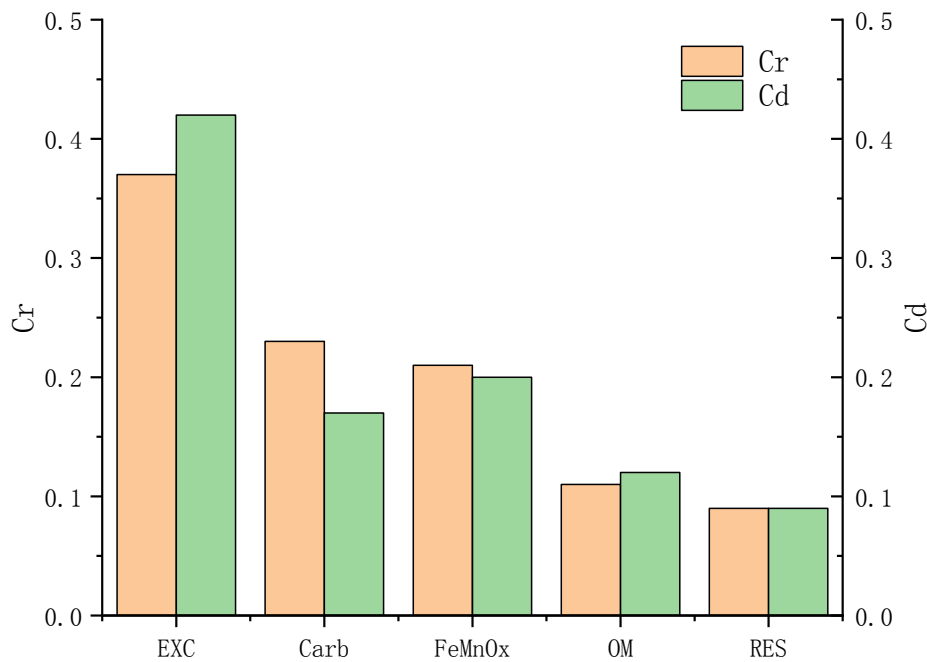


Figure 3: Morphological distribution of Cr and Cd heavy metals in aged soils

3.2 Biochar physical and chemical properties

The basic physicochemical characteristics of pine bark biochar, such as particle size distribution, pH value and elemental content, were measured at two different preparation temperatures (300°C and 600°C) as shown in Table 3, and the analysis of each basic physicochemical index of biochar is as follows.

Table 2: Biochar physical and chemical properties

	PB300	PB600
sand (%)	42.79	21.42
silt (%)	57.26	74.15
clay (%)	0.95	4.43
pH	8.84	10.00
ash content (%)	2.83	7.90
C (%)	66.20	84.60
N (%)	0.82	1.86
H (%)	4.34	1.95
O (%)	25.81	3.69
H/C	0.07	0.02
O/C	0.39	0.04
(O+N)/C	0.40	0.07

- (i) **Biochar particle size distribution.** The results of particle size distribution showed that the biochar was dominated by powder particles. As the biochar preparation temperature increased from 300°C to 600°C, the powder particle content of pine bark biochar increased from 57.26% to 74.15%, an increase of 29.50%, and a decrease in the percentage content of sand particles. A related study[18] showed that the higher the powder particle content of biochar, the more beneficial for heavy metal adsorption.
- (ii) **Biochar pH and ash content.** Biochar obtained by cracking raw biomass at a certain temperature tends to exhibit a high pH value. As seen in Table 3, the pH values of the biochars prepared at 300 and 600°C cracking conditions were 8.84 and 10.00, respectively. Both prepared biochars were alkaline and the pH values increased with the increase of cracking temperature. This occurred probably because the biomass raw material will start to produce alkaline salts continuously with the increase of temperature, which could contribute to the increase of pH. The ash content of PB300 and PB600 were 2.83% and 7.90%, respectively, which could be attributed to more mineral elements in the pine bark biochar[19] and the high cracking temperature is more likely to produce more ash.
- (iii) **Biochar elemental composition.** The results of the elemental composition of biochar were measured as shown in Table 3. As the cracking temperature of biochar preparation increased, the C content of biochar increased, and the content of H and O, the ratio of H/C, O/C and (O+N)/C decreased. This indicates that the high temperature biochar has a higher degree of carbonization. The biochar obtained at higher cracking temperatures has a larger specific surface area, thus more conducive to forming the microporous structure of biochar.[20] Biochar PB600 had the smallest H/C of 0.02, which indicates that biochar PB600 may possess a more complete degree of aromatization. The O/C and (O+N)/C of biochar PB300 were both nearly 0.40, probably because of the well polarized and hydrophilic surface of biochar PB300 with more oxygenated functional groups. Biochar PB300 contains higher H and O contents, indicating that biochar PB300 may contain more oxygen-containing surface functional groups[21]. To further verify the above speculations, XRD and FTIR analyses were performed on the two biochars.

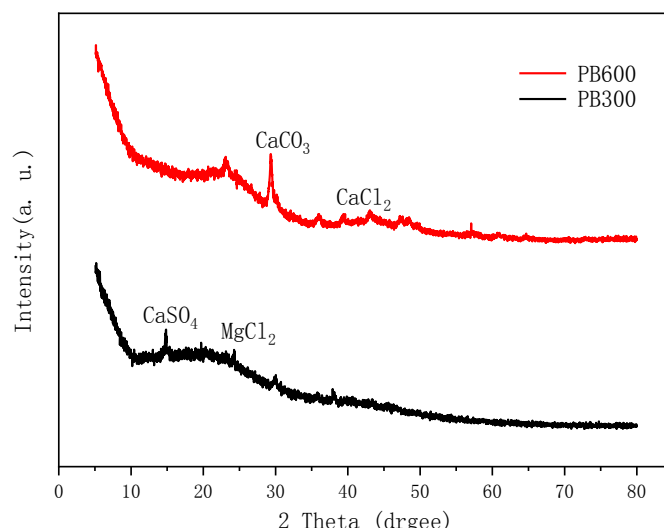


Figure 4: XRD patterns of PB300, PB600

Figure 4 shows the X-ray diffraction patterns of the two biochars prepared at cracking temperatures of 300°C and 600°C. Searches revealed that fewer diffraction peaks appeared, and none of them was obvious. PB300 showed a CaSO_4 diffraction peak near 15° and a MgCl_2 diffraction peak near 25° . In PB600, the diffraction peaks of CaCO_3 and CaCl_2 were found near 30° and 45° . Taking the above into account, the low-temperature biochar PB300 contains CaSO_4 and MgCl_2 , while the high-temperature biochar PB600 contains CaCl_2 .

Biochar's surface functional groups are determined by infrared spectroscopy. The FTIR variation can reflect the pyrolytic oxidation and water loss of biochar, etc. The determination is based on the principle that each functional group of organic matter can exhibit a specific peak within a certain wavelength of the infrared spectrum. Biochar mainly contains carbonyl ($\text{C}=\text{O}$), carboxyl ($-\text{COOH}$), hydroxyl ($-\text{OH}$), aromatic $\text{C}=\text{N}$ bond and $\text{N}-\text{H}$ bond. $3600\text{--}3100\text{ cm}^{-1}$ broad absorption peak is the $\text{O}-\text{H}$ stretching vibration; $3040\text{--}2900\text{ cm}^{-1}$ is the $\text{C}-\text{H}$ stretching vibration; $2160\text{--}2120\text{ cm}^{-1}$ is the $\text{R}-\text{N}=\text{N}=\text{N}$ stretching vibration; 1700 cm^{-1} is the $\text{R}-\text{N}=\text{N}=\text{N}$ stretching vibration. The absorption peaks at 1700 cm^{-1} are mostly $\text{C}=\text{O}$ stretching vibrations in ketones, acids and aromatic esters; the absorption peaks at $1650\text{--}1550\text{ cm}^{-1}$ are related to $\text{N}-\text{H}$ bond stretching vibrations; the stretching vibrations of $\text{C}-\text{O}$ bonds of fatty ethers and $\text{C}-\text{O}$ bonds of alcohols are at the absorption peaks around 1090 cm^{-1} ; the changes in the wave number bonds below 600 cm^{-1} may be due to the stretching vibrations of potassium chloride, calcium chloride and other inorganic compounds such as potassium chloride, calcium chloride, etc.[22]

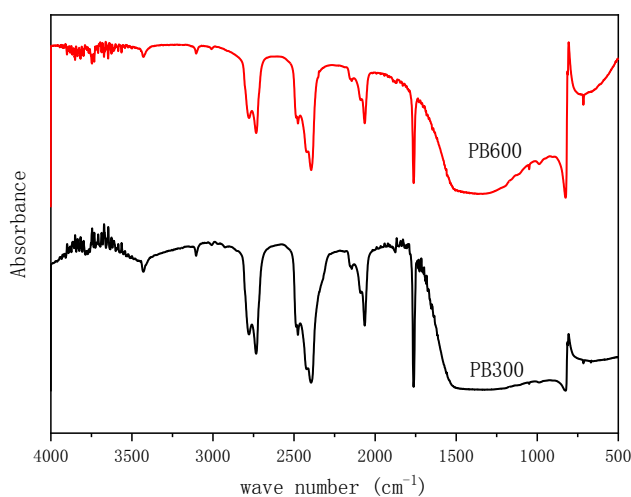


Figure 5: FTIR characterization of PB300 and PB600

Figure 5 shows the FTIR profiles of pine bark biochar at cracking temperatures of 300°C and 600°C, respectively. As shown in the figure, it was not very obvious that the change in the type and number of functional groups occurring on the surface of the biochar. The number of absorption peaks and absorbance of the biochar prepared at 600 °C were lower than that of the biochar prepared at 300 °C. This occurred probably due to the decomposition of organic compounds in the biochar as the preparation temperature increased, resulting in a decrease in the H/C, O and (O+N)/C atomic ratios, and therefore a decrease in the number of surface functional groups. The stretching change of the peak near 3450 cm⁻¹ indicates that the -OH group is located on the surface of PB. However, the reactive oxygen functional group gradually decreases with increasing temperature, indicating an intensification of the dehydrogenation reaction. the fluctuation of the peak at 1800-1000 cm⁻¹ is caused by stretching vibrations between bonds (e.g. C=C, C=O and CH₃), and the peak decreases significantly with increasing pyrolysis temperature. Owing to this, the C=O bonds are easily cleaved to generate gaseous or liquid by-products at higher thermal cleavage temperatures. Therefore, the biochar prepared at high temperature has a reduction of internal oxygen-containing functional groups such as carboxyl and carbonyl groups, despite its larger specific surface area and higher ash content. Compared with the biochar prepared at low temperatures, the high temperature preparation would reduce the complexation of heavy metals and thus the adsorption effect on heavy metals.

3.3 Longitudinal migration pattern of metal morphological changes in soil samples

As compared to the distribution of heavy metals in the blank control, the downward migration capacity of heavy metals was greatly reduced in the soil column incorporating biochar. The simulation of acid rain leaching enhanced the mobility of metals in the soil. In contrast, the soil column supplemented with biochar was able to reduce the mobility of soil metals and mitigate the effects of acid rain. Therefore, more attention to metal morphology is needed when using biochar to immobilize soil metals.

In order to further explore the morphological changes during the longitudinal migration of heavy metals, the soil samples in the column were divided at 2 cm intervals to obtain subsamples after drenching, and the obtained soil samples were extracted by the Tessier five-step sequential extraction method to obtain the contents of the five different forms of heavy metals Cr and Cd respectively.

3.3.1 Changes in Cr morphology in surface soils

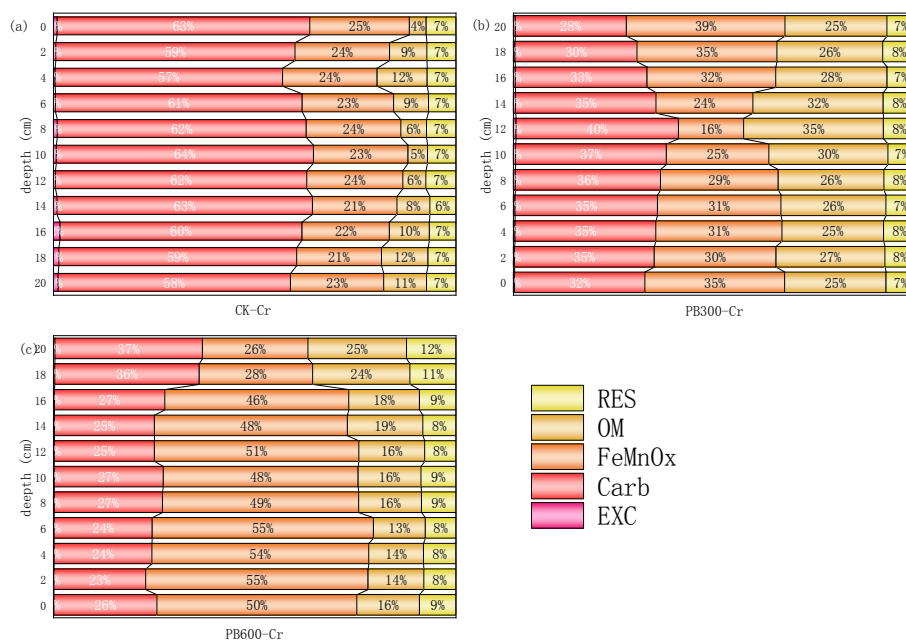


Figure 6: Morphological distribution of Cr in the surface layer of soil column

Figure 6 shows the morphological distribution of heavy metal Cr in the surface layer of the soil column. As can be seen from the figure, the morphological distribution of heavy metal Cr in the surface layer of the soil column with biochar addition was significantly different from that of the control group (surface layer of the soil column without biochar addition), and the overall consistent morphological distribution pattern was as follows: the content of the weak acid extractable state of heavy metal Cr decreased compared with the control group, and the content of the Fe-Mn oxide-bound state, organic matter-bound state and residue state increased. The weak acid extractable Cr (the sum of exchangeable Cr and carbonate bound Cr) showed an increasing then decreasing trend with the depth of the soil. At a depth of 10 cm, the corresponding weak acid extractable Cr content was 14.79 mg/kg and 11.78 mg/kg, respectively. The corresponding weak acid extractable Cr contents were 85.12 mg/kg, 19.16 mg/kg and 27.37 mg/kg at the depths of 16 cm, 12 cm and 10 cm for CK-Cr, PB300-Cr and PB600-Cr, respectively, which were closely related to acid rain saturation leaching. Under the conditions of acid rain drenching, the heavy metal Cr in the upper layer of the soil column will dissolve in the drenching solution and migrate downward with the water, resulting in a higher concentration of weak acid extractable Cr at a certain depth of the soil column. The absence of this pattern of variation in the Fe-Mn oxide-bound, organic matter-bound, and residual Cr at soil depth further suggests that the exchangeable Cr and carbonate-bound Cr contribute more to the longitudinal migration of Cr in soil.

The heavy metal Cr was effectively solidified in the soil column with biochar addition. Compared with the control group, the addition of biochar increased the proportion of Cr in the Fe-Mn oxide-bound, organic matter-bound and residual states, and the low-temperature biochar increased the proportion of Cr in the Fe-Mn oxide-bound and organic matter-bound states more significantly. The increase of Cr in the residual state was more obvious for the high temperature biochar, while the increase of Cr in the residual state was more obvious for the high temperature biochar.

3.3.2 Changes in Cd morphology in surface soils

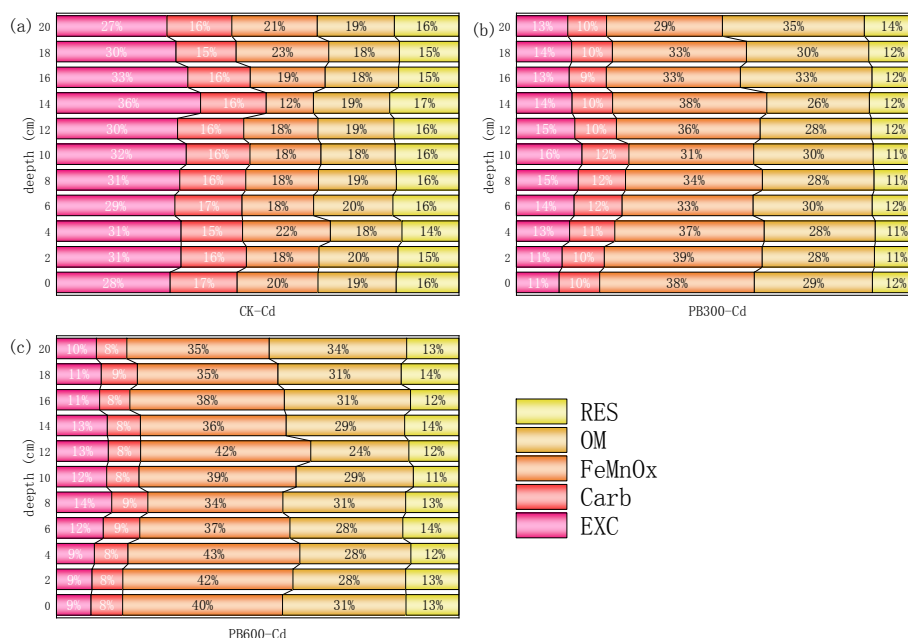


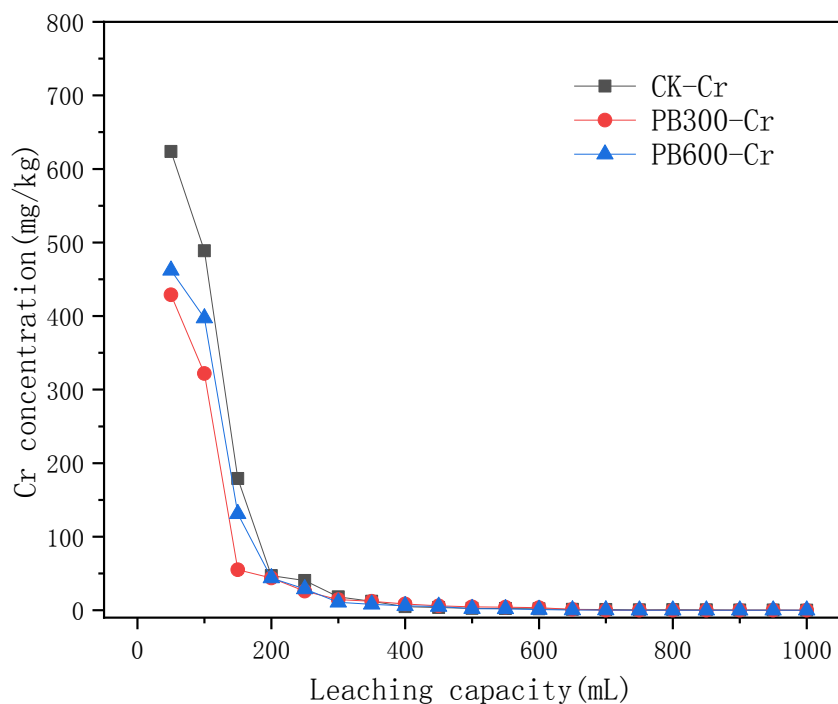
Figure 7: Variation pattern of Cd morphology with depth in the surface layer of soil columns with biochar addition

Figure 7 shows the variation pattern of Cd pattern with depth in the surface layer of the soil column with biochar addition. The average concentration of Cd in the blank soil column without biochar was 37.33 mg/kg, while the concentration of Cd in the column with biochar was 51.52 mg/kg and 52.52 mg/kg, respectively, which increased by 10 mg/kg on average compared with the control group. The biochar was able to fix heavy metals to some extent. By comparing the data of each component, we can find that compared with the control soil column CK-Cd, in the soil column with biochar added, the overall change pattern of Cd in the

surface soil was as follows: the contents of exchangeable and carbonate bound states were significantly reduced, the contents of Fe-Mn oxide-bound state and organic matter-bound state were significantly increased, and the degree of change of residue state was not obvious. This change was more obvious with the increase of the preparation temperature of the added biochar.

Similar to the Cr soil column, the weakly acid-extractable Cd showed the same trend of increasing and then decreasing in the soil column with the addition of biochar. Although this trend was not obvious in the soil column CK-Cd, the content of weakly acid-extractable Cd reached the maximum value of 18.97 mg/kg at the soil depth of 14 cm, which was probably due to the stabilization of heavy metals in the surface layer of the soil column after 14 cm of downward migration during acid rain leaching and biochar.

3.4 Changes of metal morphology in the leachate



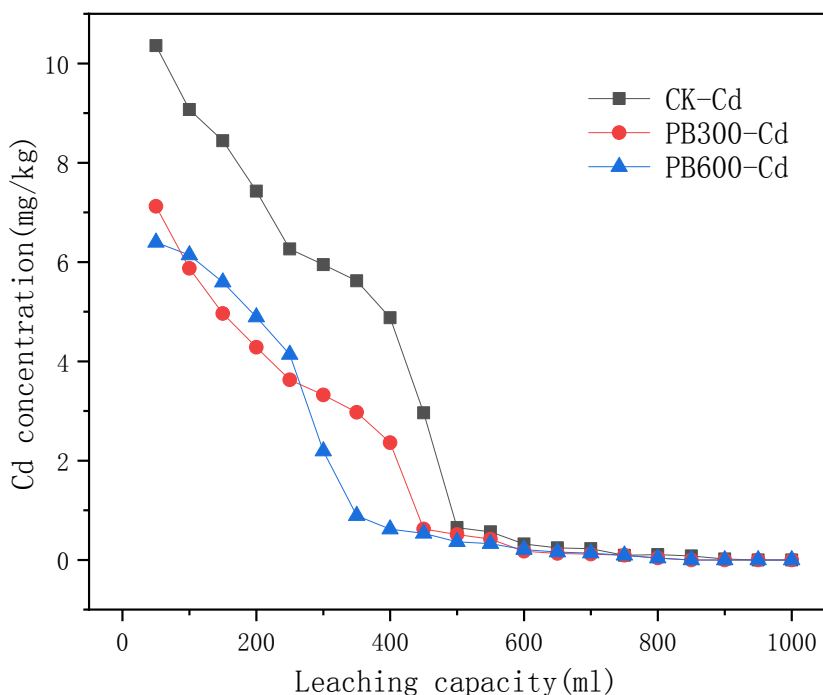


Figure 8: Accumulation of Cr and Cd in the leachate with time during the leaching process

Figure 8 shows the change of Cr metal content in the leachate with the increase of drenching volume. It can be seen from the figure that the contents of Cr and Cd in the leachate of the two untreated soils were higher than those of the leachate treated with biochar composites at the first drenching. This indicates that PB biochar had a significant passivation effect on Cr and Cd at the first drenching. The accumulation of Cr and Cd in the dewatering solution increased with the increase of drenching times. Compared with the blank control group, the increase of Cr and Cd accumulation in the PB-treated soil column dewatering solution tended to level off with time. This indicates that with the increase of drenching times, the content of mobile Cr and Cd in the soil column becomes less and less, especially in the Cd soil pollution, the passivation effect of PB600 on Cd is more obvious. The decrease of Cr and Cd concentration in the dewatering solution was larger at the beginning and then decreased significantly. This is because the water-soluble Cr and Cd at the beginning of drenching are weakly adsorbed on the surface of soil particles and are more easily released into the aqueous solution.[23] The concentration of Cr and Cd in the dewatering solution decreased gradually as the number of drenching increased and the weakly adsorbed ions were gradually lost. The accumulation of Cr and Cd in the two untreated soils still increased at a greater rate than in the treated soil column, indicating that the content of unstable forms of Cr and Cd in CK was still high.

IV. CONCLUSION

This study used pine bark as raw material to obtain four different biochar at the preparation lysis temperatures of 300°C and 600°C. Two common soil contaminated with heavy metals, Cr and Cd, were used to aging the clean soil to obtain soil contaminated with Cr and Cd singly, respectively. Then, the two biochar were added into the surface layer of soil columns contaminated with single heavy metals by using acid rain leaching simulation experiments in soil columns to explore the morphological transformation and longitudinal transport of heavy metals Cr and Cd in soil by biochar, and the following conclusions were mainly drawn.

- i. Heavy metals all have different distribution forms in the soil, which are exchangeable state, carbonate bound state, Fe-Mn oxide bound state, organic matter bound state and residue state. In the Cr-contaminated soil of this study, the exchangeable state is the main form present in the soil with 37%; in the Cd-contaminated soil, the exchangeable state Cd distribution is 42%. These two types of heavy metal contaminated soils have high contents of exchangeable and carbonate bound states[24].

- ii. Biochar was mainly powder particles, and the ash content of the two biochars differed greatly. Biochar PB600 had the highest ash content, and along with the increase of cracking temperature, the pH, ash and C content of biochar increased, while the content of H and O, and the ratios of H/C, O/C and (O+N)/C decreased. The carbonation of biochar increased and the oxygen-containing functional groups on the surface decreased. There was a correlation between the particle size difference, ash content, carbonation degree and pH of biochar on the adsorption of heavy metals.
- iii. When biochar was added to the surface soil contaminated with Cr and Cd, the total amount of heavy metals in the surface soil profile (0-20 cm) was higher than that in the control group for the same heavy metal element, and on the contrary, the total amount of heavy metals in the lower soil profile (20-40 cm) was lower than that in the control group. The biochar produced in this study had some solidification and retention effect on the heavy metal contamination of both soils tested[25]. The magnitude of the retention effect was related to the cracking temperature of biochar preparation. Within the surface layer of the Cr-contaminated soil column, the retention effect of biochar exhibited PB300 > PB600, while within the surface layer of the Cd-contaminated soil column, it showed PB600 > PB300.
- iv. Biochar can effectively reduce the content of heavy metals Cr and Cd in exchangeable and carbonate-bound states and increase the content of Fe-Mn oxide-bound state, organic matter-bound state and residue state. Biochar facilitated the conversion of soil heavy metals from exchangeable and carbonate-bound states to Fe-Mn oxide-bound state, organic matter-bound state and residue state, and reduced their migration activity in the soil. The cracking temperature of biochar preparation had a greater effect on the morphological transformation of heavy metals in soil, and the effect varied significantly among biochars for the reduction of exchangeable and carbonate-bound states and the degree of increase of Fe-Mn oxide-bound state. In Cr-contaminated soils, the effect of biochar prepared at low temperatures was higher than that of high-temperature biochar, while this effect was reversed within Cd-contaminated soils. For the organic matter-bound state, the conversion to the organic matter-bound state was more favorable for the low-temperature biochar than for the high-temperature biochar, while the degree of increase in the metal residue state was better for the high-temperature biochar than for the low-temperature biochar.
- v. Biochar can not only effectively solidify the heavy metals in the soil, but also reduce the exchangeable state and carbonate-bound state of heavy metals, which are the two forms that tend to migrate in the soil, and transform them into the Fe-Mn oxide-bound state, organic matter-bound state and residue state, which are the three forms that are more stable and less likely to migrate in the soil, so as to reduce the migration activity of heavy metal pollutants and thus The effect of stabilization is achieved. The application of biochar will also reduce the risk of leaching of soil heavy metal pollutants to groundwater, which is a practical and economical new green material for soil remediation.

REFERENCES

- [1]. Zhu limin and Feng zongwei, Study on the economic loss caused by acid deposition in forests of Jiangsu Province. *Rural Eco-Environment*, 1997(01): p. 2-5+9.
- [2]. El-Naggar, A., et al., Modified and pristine biochars for remediation of chromium contamination in soil and aquatic systems. *Chemosphere*, 2022. 303(Pt 1): p. 134942.
- [3]. Zhao, B., et al., Characterization of heavy metal desorption from road-deposited sediment under acid rain scenarios. *J Environ Sci (China)*, 2017. 51: p. 284-293.
- [4]. Guo Zhaohui, et al., Effect of blocking major exogenous inputs of heavy metals on Cd-Pb accumulation in soil-rice systems. *Transactions of the Chinese Society of Agricultural Engineering*, 2018. 34(16): p. 232-237.
- [5]. Stolpe, C., et al., Both heavy metal-amendment of soil and aphid-infestation increase Cd and Zn concentrations in phloem exudates of a metal-hyperaccumulating plant. *Phytochemistry*, 2017. 139: p. 109-117.
- [6]. Palansooriya, K.N., et al., Soil amendments for immobilization of potentially toxic elements in contaminated soils: A critical review. *Environ Int*, 2020. 134: p. 105046.
- [7]. Wang, D., et al., Biochar production and applications in agro and forestry systems: A review. *Sci Total Environ*, 2020. 723: p. 137775.
- [8]. Wang, J. and S. Wang, Preparation, modification and environmental application of biochar: A review. *Journal of Cleaner Production*, 2019. 227: p. 1002-1022.
- [9]. Rizwan, M., et al., Mechanisms of biochar-mediated alleviation of toxicity of trace elements in plants: a critical review. *Environ Sci Pollut Res Int*, 2016. 23(3): p. 2230-48.
- [10]. El-Naggar, A., et al., Biochar composition-dependent impacts on soil nutrient release, carbon mineralization, and potential environmental risk: A review. *J Environ Manage*, 2019. 241: p. 458-467.
- [11]. Li Xiaohui, Study on passivation effect of new modified rice husk biochar materials on cadmium contaminated soil. *Ecology and Environmental Sciences*, 2022.
- [12]. Liao Yueqing, et al., Leaching Effect of Biochar and Zeolite on Pb, Cd and W in Tungsten Ore Area of Jiangxi Province Under Simulated Acid Rain Conditions. *Journal of Soil and Water Conservation*, 2021. 35(06): p. 319-326.

- [13]. Tao Quan, et al., Leaching Effects of Modified Zeolite on Pb and Zn in Contaminated Soil Under the Condition of Simulated Acid Rain. *Journal of Soil and Water Conservation*, 2015. 29(05): p. 304-308.
- [14]. Hu Fangjie, et al., Leaching Effects of Lead-contaminated Farmland by Simulated Acid Rain. *Bulletin of Soil and Water Conservation*, 2019. 39(03): p. 170-174.
- [15]. Tessier, A., Sequential Extraction Procedure for the Speciation of Particulate Trace Metals. *ANALYTICAL CHEMISTRY*, 1979.
- [16]. Wang Miaomiao, Progress of using biochar in remediation of heavy metal polluted soil. *Applied Chemical Industry*, 2022.
- [17]. Gao Xuefang, Study on improvement of ring knife method for determining soil field water capacity. *Ningxia Engineering Technology*, 2019.
- [18]. Meng Lingyang, Effects of Materials Containing Different Inert Organic Carbon on Cd Speciation and Bio-Availability in Soil. *Journal of Agro-Environment Science*, 2011.
- [19]. Chu Yingchao, Adsorption of Cd(II) , As(III) , Cr(III) and Cr(VI) by coconut fiber-derived biochars. *Chinese Journal of Environmental Engineering*, 2015.
- [20]. Yuan, J.H., R.K. Xu, and H. Zhang, The forms of alkalis in the biochar produced from crop residues at different temperatures. *Bioresour Technol*, 2011. 102(3): p. 3488-97.
- [21]. Liu Jiming, Remediation effect of solidification/stabilization of several mineral materials on a heavy metal contaminated farmland soil. 2017, Nanjing Forestry University.
- [22]. Wang, Z., et al., Characterization and influence of biochars on nitrous oxide emission from agricultural soil. *Environ Pollut*, 2013. 174: p. 289-96.
- [23]. Li, P., Applying modified biochar with nZVI/nFe₃O₄ to immobilize Pb in contaminated soil. *Environmental Science and Pollution Research*, 2020.
- [24]. Li Zhen, et al., Washing efficiency of Cd from contaminated Lou soil by saponin and low-molecular-weight organic acids. *Journal of Northwest A&F University(Nat, Sci, Ed.)*, 2018. 46(05): p. 85-93+100.
- [25]. Xiang yang, et al., Influence of Biochar on Accumulation of Soil Cd and Pb in and Physiological Characteristics of *Lonicera japonica*. *Agricultural Science & Technology*, 2021. 22(02): p. 45-50.